

Supplementary Information

Ir Nanoclusters/Porous N-Doped Carbon as Bifunctional Electrocatalyst for Hydrogen Evolution and Hydrazine Oxidation Reactions

Hong-Li Huang,[#] Xiya Guan,[#] Haibo Li, Ruiqing Li, Rui Li, Suyuan Zeng, Shuo Tao, Qingxia Yao, Hongyan Chen and Konggang Qu*

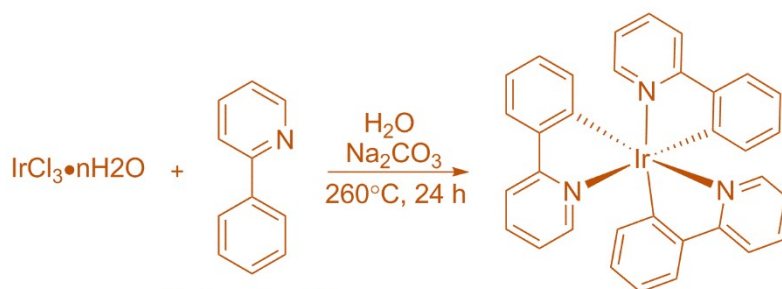
School of Chemistry and Chemical Engineering, Shandong Provincial Key Laboratory/Collaborative Innovation Center of Chemical Energy Storage & Novel Cell Technology, Liaocheng University, Liaocheng 252059, China
Email: qukonggang@lcu.edu.cn

1. Experimental

1.1 Materials

$\text{IrCl}_3 \cdot n\text{H}_2\text{O}$, 2-phenylpyridine, and silica nanoparticles were purchased from Aladdin Industrial Corporation (Shanghai, China). The commercial 20% Pt/C was provided by Shanghai Hesen Corporation. The commercial 20% Ir/C was purchased from Premetek Co.

1.2 Synthesis



Tris(2-phenylpyridine)iridium ($\text{Ir}(\text{ppy})_3$) was synthesized according to the literature.¹ To a two necked, 500 mL round bottom flask equipped with a magnetic stir bar were added iridium (III) chloride (192 mg, 0.64 mmol), 2-phenylpyridine (1.19 g, 7.7 mmol), Na_2CO_3 (407 mg, 3.8 mmol), and distilled water (213 mL). The mixture was degassed with Ar for 15 min and then heated to 260°C for 24 h. After cooling to room temperature, reaction mixture was extracted with DCM (3×250 mL). The organic layer was combined, dried (MgSO_4), filtered, and concentrated in vacuo. The resulting residue was purified by column chromatography (DCM) to afford the desired $\text{Ir}(\text{ppy})_3$ in 79% yield (311 mg, 0.47 mmol) as a yellow solid.

200 mg $\text{Ir}(\text{ppy})_3$ was added into 90 mL ethyl alcohol. Then silica powder (SiO_2 , 1.6 g) was added, and further dispersed to form a homogeneous yellow solution. The mixture was stirred overnight and dried by rotary evaporation. The obtained powder was pyrolyzed under 700°C for 3 h in a tube furnace with a heating rate of 5°C min^{-1} at Ar atmosphere, to yield silica-templated Ir/PNC. To remove the silica template, the composite material was placed into a freshly prepared solution containing hydrofluoric acid aqueous solution and stirred for 6 h.² After the materials were washed repeatedly by centrifugation. The resultant Ir/PNC were dried in vacuum oven at 80°C for 18 h. The content of Ir is 15.0 wt% determined with inductively coupled plasma optical

emission spectrometer (ICP-OES).

Meanwhile, Ir/N-doped carbon material (Ir/NC) was prepared following the same procedure as Ir/PNC without silica nanoparticles with 17.3 wt% Ir loading determined by ICP-OES.

1.3 Characterizations

The morphology and structure were examined by the transmission electron microscope (TEM, Talos F200X G2), powder X-ray diffraction (XRD, SmartLab 9kW) and Raman spectrometer with an excitation wavelength of 532 nm (HORIBA iHR550). The component information was obtained by TEM energy-dispersive X-ray spectroscopy (EDS) mapping and X-ray photoelectron spectroscopy (XPS, Kratos Axis Ultra spectrometer). The specific surface areas were extracted with nitrogen adsorption-desorption isotherm (Micrometrics Tristar II) by the Brunauer-Emmett-Teller (BET) model at a pressure range of $P/P_0 = 0.05-0.3$, along with the Barrett-Joyner-Halenda (BJH) model for pore size distribution by the adsorption branch on isotherm. ICP-OES was performed with PerkinElmer Optima 8300.

1.4 Electrocatalytic experiments

The electrochemical station (Reference 3000, Gamry Instruments, USA) with a rotating disk electrode (RDE) system were used to conduct the electrochemical measurements. For the preparation of working electrode, the samples were initially ultrasonically dispersed into aqueous inks with the concentration of 2 mg mL^{-1} . $20 \mu\text{L}$ of the catalyst ink was dropped onto a pre-prepared RDE with the diameter of 5 mm and dried at ambient condition, then $5 \mu\text{L}$ of 0.5 wt. % Nafion aqueous solution was added to increase the adherence. An Ag/AgCl/KCl (3.5 M) electrode and a graphitic carbon was selected as the reference and counter electrodes, the volume of 100 mL electrolyte was added into a 5-port electrolytic cell with N_2 gas inlet during the tests. The equation $E_{\text{RHE}} = E_{\text{Ag/AgCl}} + (0.205 + 0.059 \text{ pH}) \text{ V}$ was used to calibrate the potentials.

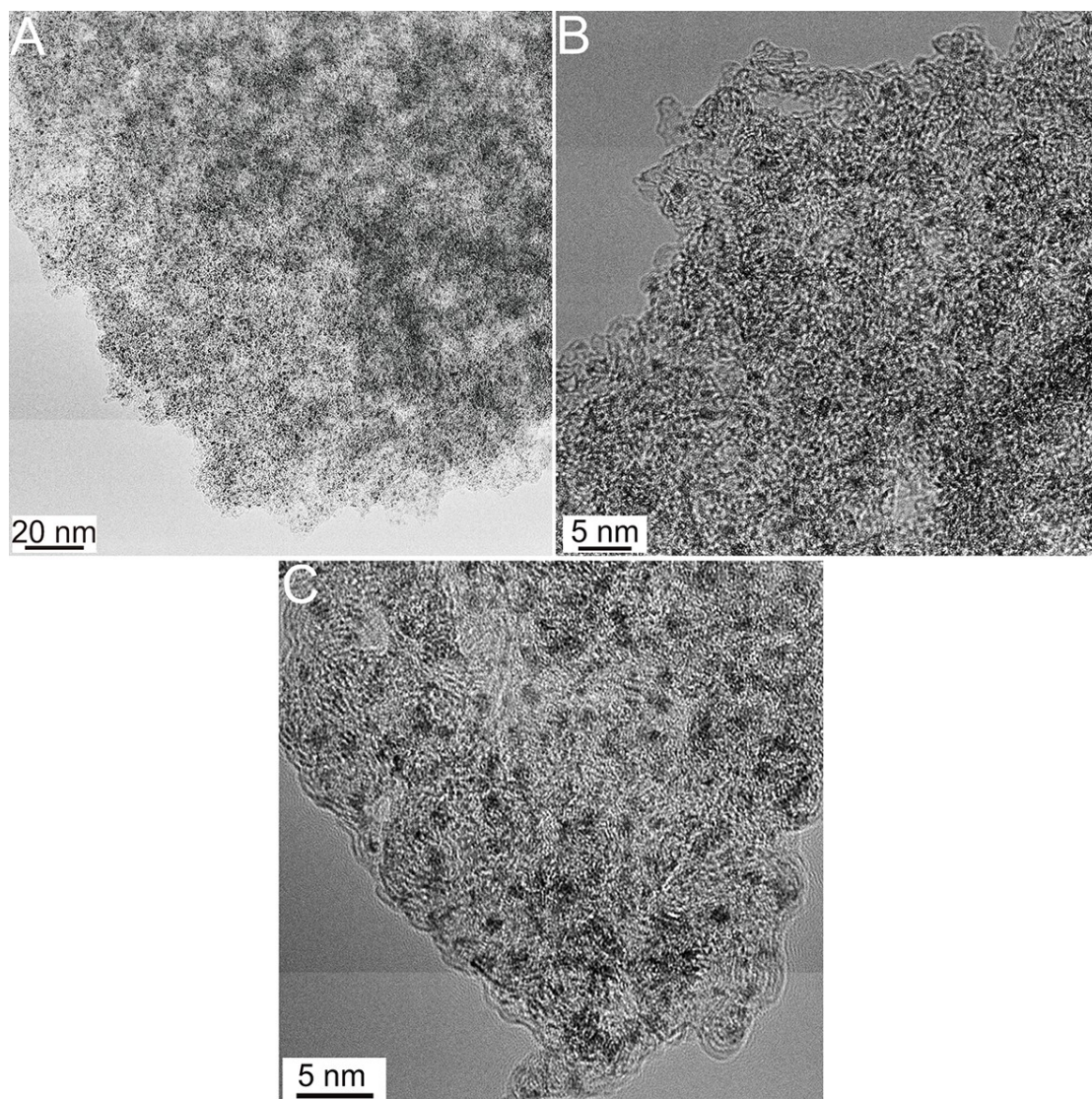


Fig. S1 TEM images of Ir/PNC at different magnifications.

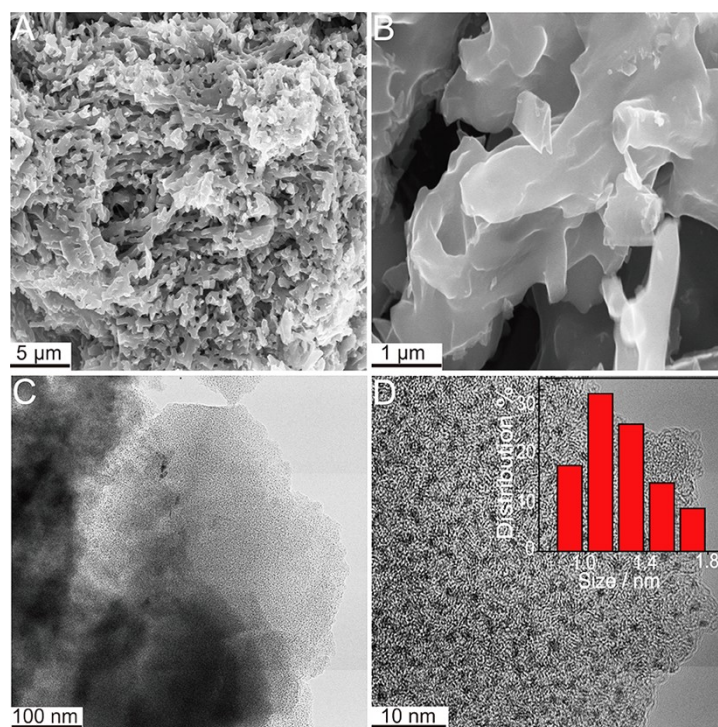


Fig. S2 (A, B) SEM images of Ir/NC at different magnifications. (C, D) TEM images of Ir/NC at different magnifications, Inset: The corresponding Ir size distribution for Ir/NC.

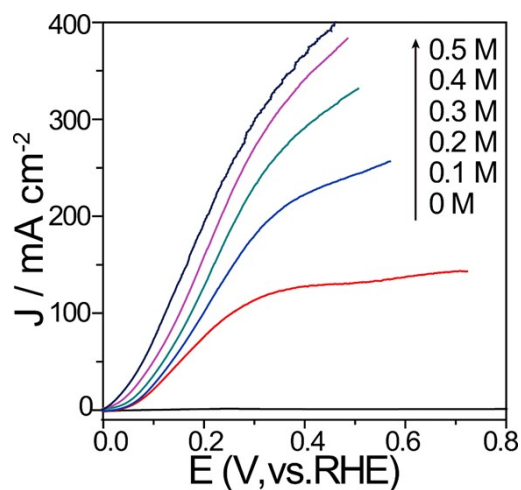


Fig. S3 LSV curves of Ir/PNC in 1.0 M KOH containing different concentrations of N_2H_4 .

As shown in Fig. S3, negligible anodic current was produced in the potential range of 0~0.8 V (vs. RHE) without hydrazine. In contrast, the anodic current density increases strongly with the progressive addition of 0.1~0.3 M N_2H_4 and while only rises slightly with the concentration of N_2H_4 up to 0.4~0.5 M. Therefore, 1.0 M KOH containing 0.5 M N_2H_4 was chosen as the electrolyte for HzOR.

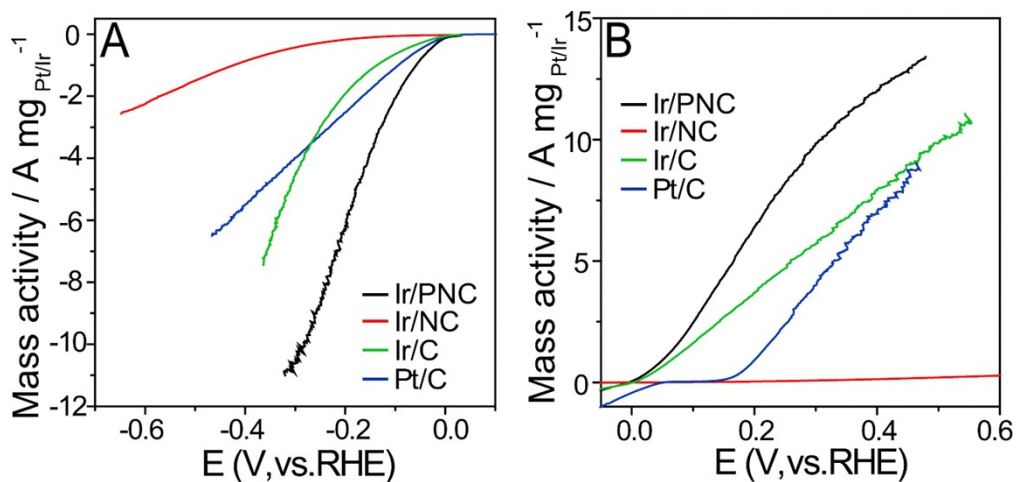


Fig. S4. Mass activity of different catalysts for (A) HER and (B) HzOR.

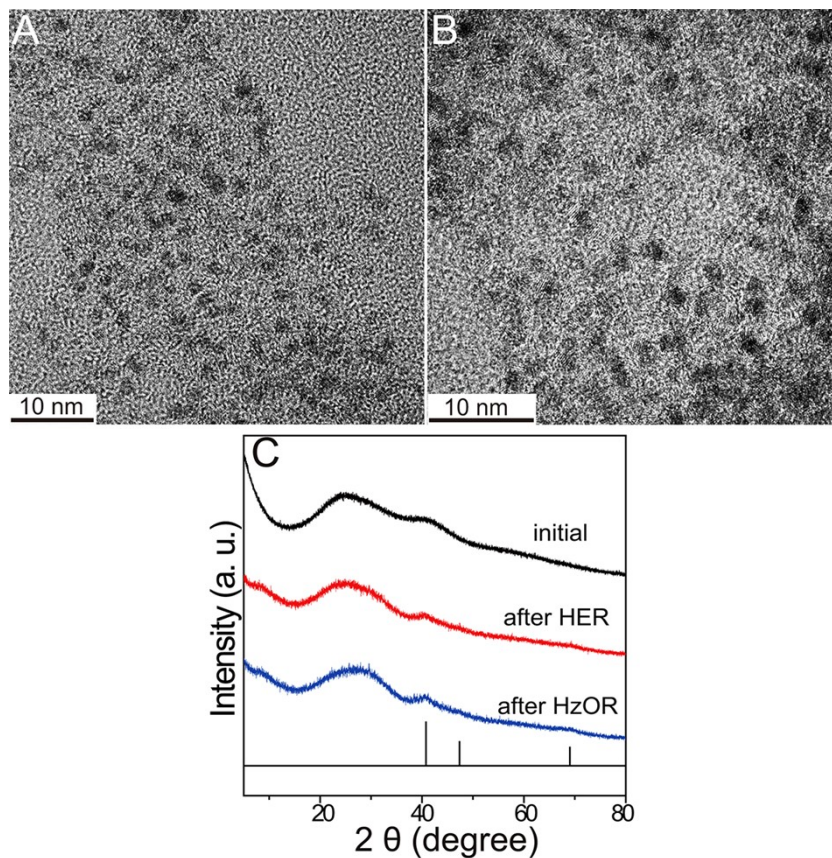


Fig. S5. The TEM images of Ir/PNC after 10 h's stability test for (A) HER and (B) HzOR, respectively. (C) The compared XRD patterns of initial Ir/PNC and after 10 h's stability test for HER and HzOR.

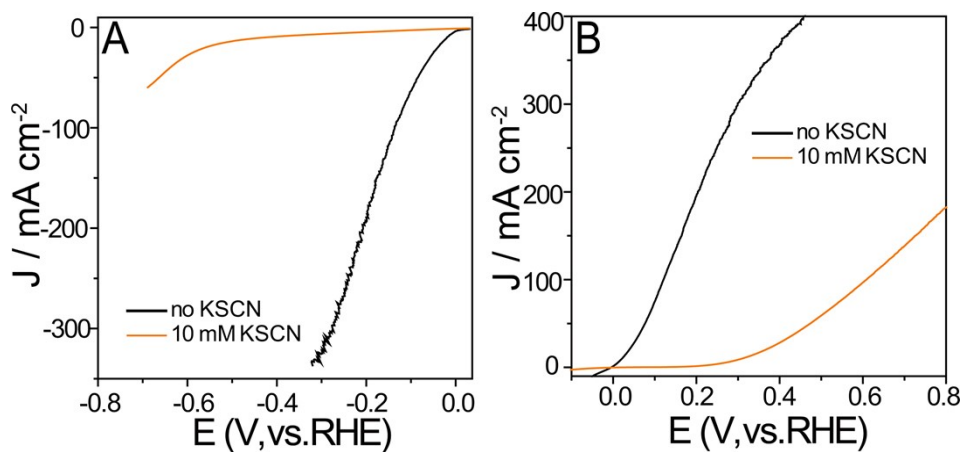


Fig. S6 The poison test of SCN^- . LSV curves for (A) HER and (B) HzOR.

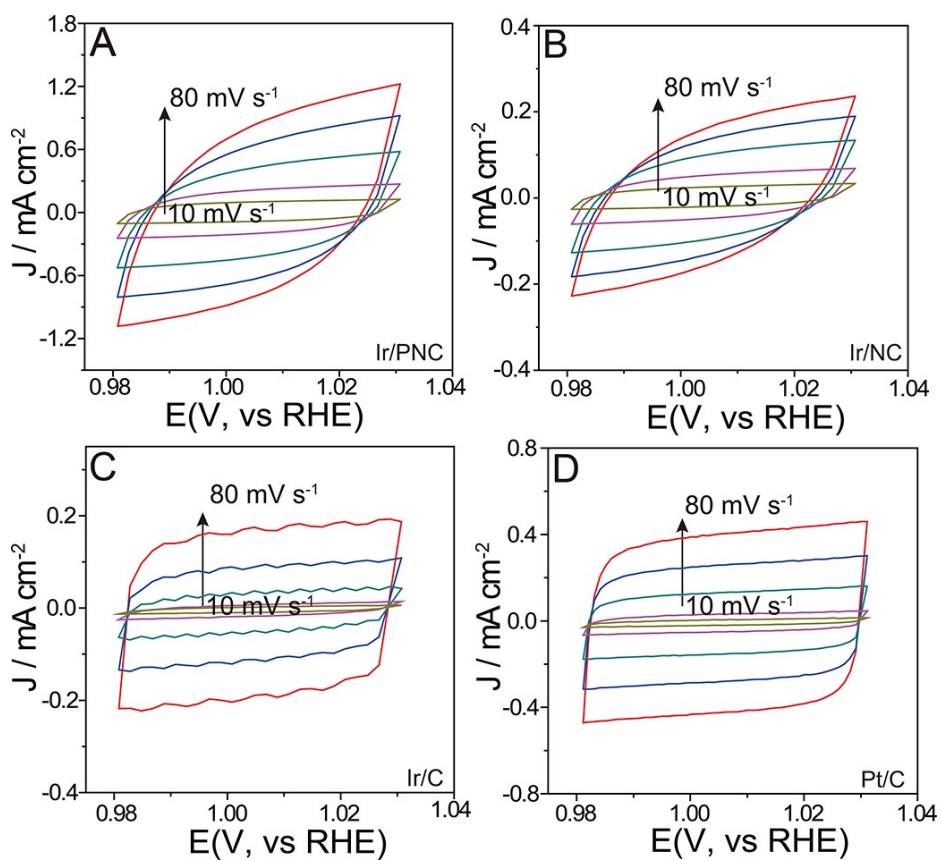


Fig. S7 CV curves at different scan rates (10, 20, 40, 60, 80 and 100 mV s^{-1}) of catalysts of (A) Ir/NPC, (B) Ir/NC, (C) Ir/C and (D) Pt/C.

Table S1. Quantitative XPS information of different samples.

Sample	N (at%)					Ir (at%)		C (at%)	O (at%)
	total N	Graphitic N	Pyrolic N	Ir-N	Pyridinic N	Ir	Ir-O		
Ir/PNC	6.77	2.83	1.58	1.53	0.83	1.58	1.32	74.65	15.68
Ir/NC	5.33	1.61	1.41	1.15	1.16	1.38	0.36	81.6	11.33

Table S2 Comparison on the activity of the reported Ir-based HER catalysts in alkaline electrolyte.

Materials	η_{10} (mV)	Tafel slope (mV dec ⁻¹)	References
Ir/PNC	19.8	45.5	This work
RhIr MNs	20	30.7	<i>J. Mater. Chem. A</i> , 2021, 9, 18323.
Ir-NR/C	42	35.2	<i>Appl. Catal., B-Environ.</i> , 2020, 279, 119394.
3%Ir-NCNSs	125	107	<i>ACS Appl. Mater. Inter.</i> , 2021, 13, 22448.
Ir/CN	12	28	<i>ACS Appl. Mater. Inter.</i> , 2018, 10, 22340.
RuIr@NrC	28	35	<i>Chem. Eng. J.</i> , 2021, 417, 128105.
IrP ₂ @NC	28	50	<i>Energy Environ. Sci.</i> , 2019, 12, 952.
IrP ₂ @NPC	42	56	<i>J. Mater. Chem. A</i> , 2021, 9, 2195.
Ir@CON	13.5	29	<i>Adv. Mater.</i> , 2018, 30, 1805606.
CBC-Ir-800-1.2	33	42.1	<i>Adv. Funct. Mater.</i> , 2021, 2105562.
IrP ₂ -CNFs	19	20	<i>Appl. Surf. Sci.</i> , 2021, 565, 150461.
Co@Ir/NC-10%	121	73.8	<i>ACS Sustainable Chem. Eng.</i> , 2018, 6, 5105.
Ir/MoS ₂	44	32	<i>ACS Energy Lett.</i> , 2019, 4, 368.
PdIr UNWs/WFG	23	38.4	<i>Nanoscale</i> , 2019, 11, 14561.
AC-SrIrO ₃	139	49	<i>Chem. Mater.</i> , 2020, 32, 4509.
Ni _{0.93} Ir _{0.07} /rGO	32.5	64.3	<i>J. Energy Chem.</i> , 2020, 49, 166.
Ir ₁ @Co/NC	55	119	<i>Angew. Chem., Int. Ed.</i> , 2019, 58, 11868.
IrW nanobranches	29	71.2	<i>Nanoscale</i> , 2019, 11, 8898.
Ir_VG	17	29	<i>J. Mater. Chem. A</i> , 2019, 7, 20590.
Ir-NSG	18.5	28.3	<i>Nat. Commun.</i> , 2020, 11, 4246.
Ir/CeO ₂	36	33.3	<i>Chem. Commun.</i> , 2021, 57, 8798.
Ir@NG-750	114	113	<i>J. Mater. Chem. A</i> , 2020, 8, 19665
Ir/VC/C-100	22	45.2	<i>Chem. Commun.</i> , 2021, 57, 10395.
Ir/CNT/rGO	19	32	<i>Sustain. Energ. Fuels</i> , 2020, 4, 3288.
Ir ₁₆ -PdCu/C	99	90.3	<i>Nano Lett.</i> , 2021, 21, 5774.
Ni/np-Ir	20	23	<i>ACS Nano</i> , 2021, 15, 5333.

Supplementary References

1. A. Singh, K. Teegardin, M. Kelly, K. S. Prasad, S. Krishnan, J. D. Weaver, *J. Organomet. Chem.*, 2015, **776**, 51.
2. L. Zhang, P. Wang, W. Zheng, X. Jiang, *J. Mater. Chem. B.*, 2017, **5**, 6601.
3. Y. Xie, X. Long, X. Li, C. Chang, K. Qu, Z. Yang, *Chem. Commun.*, 2021, **57**, 8620.